



A Wedge-Shaped Au Thin Film: Integrating Multiple Surface Plasmon Resonance Sensors in a Single Chip and Enhancing the Figure of Merit

Hiromasa Shimizu^{1,2*}, Takahiro Ogura¹, Takumi Maeda¹ and Shogo Suzuki¹

¹Department of Electrical and Electronic Engineering, Tokyo University of Agriculture and Technology, Koganei, Japan,

²Department of Applied Physics and Chemical Engineering, Tokyo University of Agriculture and Technology, Koganei, Japan

We show here the design, fabrication, and characterization of a wedge-shaped Au thin film with an enhanced figure of merit (FOM). This is achieved by using a reflectivity change in an attenuated total reflection (ATR) setup by slightly modulating the wavenumber of the surface plasmon polariton by means of the varying thickness of the Au thin film. The wedge-shaped Au thin film is equivalent to multiple surface plasmon resonance (SPR) transducers integrated in a single chip and was fabricated by an electron-beam evaporation process with the position of the shutter controlled during the deposition. The FOM, defined as the difference between the maximum and minimum values of the normalized reflectivity change ($\Delta R/R$) divided by the corresponding difference of the incident angles, was 8.0-times larger than that based on the reflectivity R . Also, we demonstrated that the wedge-shaped Au thin film was able to detect ethanol gas at a concentration of 0.2%, corresponding to a refractive index change of 2×10^{-5} , without any surface functionalization. Since the sensing signal can be obtained with a single image from the wedge-shaped Au thin film without precise thickness control of the metal thickness, no other materials or modulation equipment is necessary, and the sensing chip can be employed in simple and highly sensitive systems.

Keywords: surface plasmon resonance, figure of merit, wedge-shaped film, refractive index sensing, gas detection

OPEN ACCESS

Edited by:

Maria Laura Ermini,
Italian Institute of Technology (IIT), Italy

Reviewed by:

Raj Kumar Gupta,
Birla Institute of Technology and
Science, India
Linhan Lin,
Tsinghua University, China

*Correspondence:

Hiromasa Shimizu
h-shmz@cc.tuat.ac.jp

Specialty section:

This article was submitted to
Nanomaterials,
a section of the journal
Frontiers in Nanotechnology

Received: 13 June 2021

Accepted: 16 September 2021

Published: 15 October 2021

Citation:

Shimizu H, Ogura T, Maeda T and
Suzuki S (2021) A Wedge-Shaped Au
Thin Film: Integrating Multiple Surface
Plasmon Resonance Sensors in a
Single Chip and Enhancing the Figure
of Merit.
Front. Nanotechnol. 3:724528.
doi: 10.3389/fnano.2021.724528

INTRODUCTION

Surface plasmon resonance (SPR) sensors are powerful tools for real-time highly sensitive and label-free detection of analytes with a small size and high throughput, and have been applied to biomolecule (protein, DNA) detection by monitoring the change in the refractive index (RI) on the metal surface (Liedberg et al., 1983; Liedberg et al., 1995; Homola et al., 1999; Phillips, 2008). Higher sensitivity has been required in order to measure a smaller change in the RI by smaller molecules such as gas molecules for applications in the field of security, healthcare, biomedical applications, environmental monitoring, agriculture, and food industry. A lot of approaches have been studied in SPR sensors built on propagating plasmonic eigenwave, surface plasmon polariton (SPP), or localized plasmonic eigenmode, localized surface plasmon resonance (LSPR).

Modulation of SPP by, for example, mechanical (Patskovsky et al., 2008; Shin et al., 2010), phase (Markowicz et al., 2007; Kabashin et al., 2009), and magneto-optic (MO) modulation (Sepúlveda et al., 2006; Regatos et al., 2010; Regatos et al., 2011; Manera et al., 2014; Maccaferri et al., 2015; David et al., 2015; Herreno-Fierro et al., 2016; Kaihara et al., 2019), is effective in improving the RI

sensitivity, signal-to-noise ratio (SNR), and limit of detection (LOD). For these modulation configurations, external modulators are necessary leading to large-size, high-cost, and complex sensor systems. Preparation of the metal multilayer including nonmagnetic and ferromagnetic metals is necessary in SPR sensors with magneto-optic modulation. Small-size, low-cost, and simple SPR sensors without precise thickness of control of the metal film are desired. However, reports on SPR sensors satisfying these demands are limited.

We have reported modulation of surface plasmon resonance by magnetization reversal in Au/Fe/Au trilayer for achieving higher refractive index sensitivity (Suzuki et al., 2021). Instead of introducing a ferromagnetic layer, changing the metal layer thickness is effective for modulating the wavenumber of SPP without excess loss due to the ferromagnetic metal. We demonstrated SPR transducers with a wedge-shaped membrane structure on an Au thin film in the Otto configuration (Shimodaira et al., 2019). The transducers are formed of a membrane, where the space for the analyte is sandwiched between SiO₂ and Au thin films, fabricated by wafer bonding of an SiO₂ substrate on an Au thin film deposited on a Si substrate *via* ball spacers to define the thickness (t) of the space for the analyte. We confirmed the modulation of the surface plasmon resonance by observing the incident angle dependence of the reflectivity for a fixed wavelength of 1,550 nm with a focusing lens and an infrared camera. We obtained images of different positions having different t , where t is modulated owing to the inhomogeneous bonding force. From the difference of the asymmetric intensity distributions of the images from different positions, multiple SPR transducers with wedge membrane structures on the Au thin film to achieve modulation of SPP were demonstrated in a single transducer without using external modulators or an electromagnet. In sensor structures with the Otto configuration, an RI change of the analyte in a narrow space with a thickness of $t \sim 2\text{--}3\ \mu\text{m}$ must be detected, so that the introduction of the analyte to the narrow space is an issue for practical applications. Modulating SPP by changing the metal thickness in the Kretschmann configuration enables the detection of analytes on the metal surface by controlling the metal layer thickness within 1 nm (Suzuki et al., 2021).

In this paper, we report the design, fabrication, and characterization of a wedge-shaped Au thin film, where the Au thickness (t_{Au}) varies in a single sensor chip for modulating the wavenumber, enhancing the figure of merit (FOM) for RI detection in an ATR setup. The FOM, based on the reflectivity change $\Delta R/R$ of the wedge-shaped Au thin film, was 8.0 times larger than that based on the reflectivity R . We demonstrated that the SPR sensor based on the wedge-shaped Au thin film was able to detect ethanol gas at a concentration of 0.2%, corresponding to a refractive index change of 2×10^{-5} , without any surface functionalization. Since the sensing signal can be obtained with a single image, and no other materials or modulation equipment are necessary for modulating the wavenumber, the sensing chip can be employed for simple and highly sensitive systems.

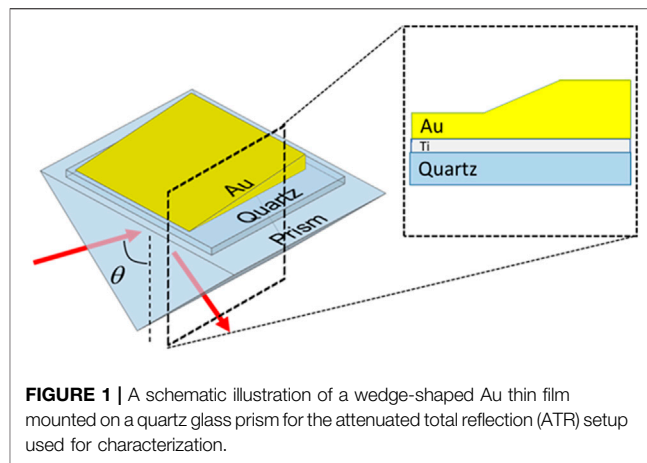


FIGURE 1 | A schematic illustration of a wedge-shaped Au thin film mounted on a quartz glass prism for the attenuated total reflection (ATR) setup used for characterization.

DESIGN AND FABRICATION OF SURFACE PLASMON RESONANCE SENSOR WITH WEDGE-SHAPED AU THIN FILM

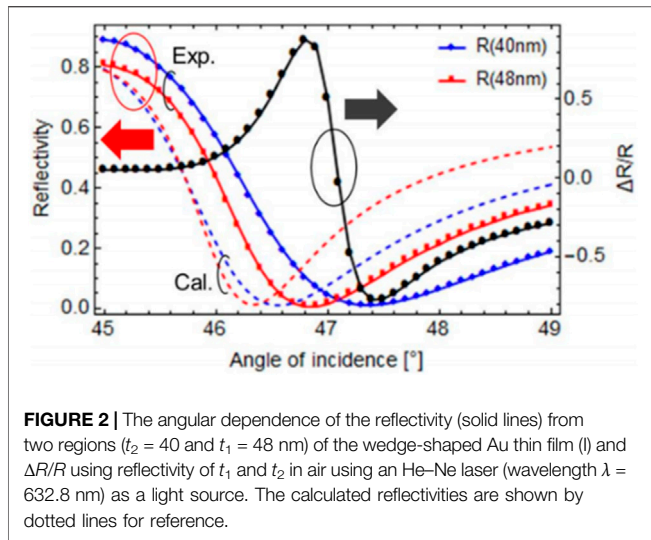
Angular Dependence of Reflectivity in the Wedge-Shaped Au Thin Film in Attenuated Total Reflection Setup

We prepared a wedge-shaped Au thin film on a quartz glass substrate mounted on a right-angle quartz prism, as schematically shown in **Figure 1**, based on the calculated incident angle dependence of the reflectivity. The RI of a dielectric on the Au film was set at 1 for gas-sensing applications. Based on our previous study (Suzuki et al., 2021), the minimum reflectivity satisfying the momentum matching condition was obtained when the Au layer thickness was 44 nm. Based on simulations, the minimum and maximum thicknesses were set at 40 and 48 nm, which includes the Au layer thickness of 44 nm. First, we prepared a wedge-shaped Au thin film (I) by electron beam (EB) evaporation. A 3-nm-thick Ti thin film and a 40-nm-thick Au thin film were deposited on the whole glass substrate (15 mm \times 15 mm). Then, half of the area of the substrate was covered by the shutter inside the chamber, and an additional 8-nm-thick Au layer was deposited, so that the largest and smallest thicknesses were set at 40 and 48 nm.

Figure 2 shows the angular dependence of the reflectivity from the two regions ($t_2 = 40$ and $t_1 = 48$ nm) in air using a He–Ne laser (wavelength $\lambda = 632.8$ nm) as a light source. As the sensing magnitude, we defined the reflectivity change $\Delta R/R$ by:

$$\frac{\Delta R}{R} = \frac{R(t_2) - R(t_1)}{R(t_2) + R(t_1)} \quad (1)$$

The maximum $\Delta R/R$ was 0.868, which is close to the value of the double dielectrics and ferromagnetic metal (DDFM) structure (Kaihara et al., 2016; Kaihara et al., 2019). We defined the FOM based on **Eq. 2** as the difference between the maximum and minimum values divided by the corresponding difference of the incident angles in order to compare the sharpness of the reflectivity R and $\Delta R/R$.



$$\left\{ \left(\Delta R/R \right)_{\max, \theta_2} - \left(\Delta R/R \right)_{\min, \theta_1} \right\} / (\theta_2 - \theta_1) \quad (2)$$

For the Au thin film section of $t_1 = 48$ nm, the maximum reflectivity R_{\max} was 0.813 at $\theta = 45^\circ$, and minimum reflectivity R_{\min} was 0.0174 at $\theta = 46.9^\circ$, so that FOM was $0.34^{\circ-1}$ for reflectivity R . On the other hand, the maximum reflectivity change $(\Delta R/R)_{\max, \theta_2}$ was 0.868 at $\theta = 46.8^\circ$, and the minimum reflectivity change $(\Delta R/R)_{\min, \theta_1}$ was -0.761 at $\theta = 47.4^\circ$, so that FOM was $2.7^{\circ-1}$ for reflectivity change $\Delta R/R$. The FOM (sharpness) of $\Delta R/R$ was 8.0 times larger than that of R . It is important to reduce the reflectivity at a certain thickness t_1 for enhancing $\Delta R/R$ to ± 1 and the FOM, based on Eq. 2. It was reported that a reflectivity of 10^{-5} was realized by tuning the dielectric SiO_2 layer thickness and wavelength of the incident light (Kaiharu et al., 2016). Furthermore, thickness control of an Au layer to 1 nm or smaller is required for finding the optimum Au layer thickness t_1 . To obtain the optimum t_1 with higher thickness resolution in the Au thin film and improve the sharpness (Suzuki et al., 2021), we fabricated a wedge-shaped Au thin film and obtained the angular dependence of the reflectivity with a single image, as described in the next section.

Angular Dependence of Reflectivity in the Wedge-Shaped Au Thin Film in Attenuated Total Reflection Setup Based on Surface Plasmon Resonance Image

In order to improve the FOM, it is important to find the position showing the minimum reflectivity within the wedge-shaped Au thin film. We prepared another wedge-shaped Au thin film II ($t_{\text{Au}}: 40\text{--}50$ nm) by EB evaporation. Details of the preparation process were reported in our previous paper (Suzuki et al., 2021). We measured the thickness of the wedge-shaped Au thin film II by a stylus profiler. The smallest thickness was 34 nm, which was measured at one edge of the substrate, and smaller than the designed smallest thickness of $t_{\text{Au}} = 40$ nm. The largest thickness

was 48 nm, which was measured at the other edge, and smaller than the designed largest thickness of $t_{\text{Au}} = 50$ nm. The reason for the thickness difference is that the deposited film thickness is slightly smaller than the designed thickness and Au film deposited by EB evaporation contains the inhomogeneity of the thickness within the glass substrate ($15 \text{ mm} \times 15 \text{ mm}$). The reflectivity was measured by a CMOS camera ($2,448 \times 2,048$ pixels, 16 bits) equipped with a cylindrical focusing lens (focal length: 30 mm) for measuring the incident angle dependence of the reflectivity in air with a single image, as shown in Figure 3. A light-emitting diode ($\lambda = 632$ nm) was used as a light source, with a band pass filter having a bandwidth of 1 nm. The conversion factor from pixels to incident angle was estimated to be $0.005^\circ/\text{pixel}$ by slightly rotating the sample with a stepping motor. Figure 4 shows the luminance distribution from the wedge-shaped Au thin film. A dark area can be found between the bright areas, corresponding to the minimum reflectivity. With increasing t_{Au} , the position of the dark area shifted toward a smaller x (incident angle). Figure 5 shows the reflected light intensity along the x direction at $y = 950, 1,000, 1,050$, and $1,100$. The minimum reflectivity was observed at $y = 950$ and monotonically increased with increasing y from 950 to 1,100 (designed thickness $t_{\text{Au}} = 40\text{--}50$ nm). The thickness showing the minimum reflectivity was smaller than the minimum designed thickness ($t_2 = 40$ nm) of the wedge-shaped Au film (II). Therefore, the deposited Au layer thickness in the wedge-shaped Au thin film (II) was slightly larger than that of (I). The reflected light intensity and $\Delta R/R$ are plotted in Figure 6 based on the luminance distributions of $y = 950, 1,000, 1,050$, and $1,100$ in Figure 5. The difference of maximum and minimum reflectivity change was largest for the combination of the luminance distributions of $y = 950$ and $1,100$, owing to the largest difference of the minimum reflectivity. When the luminance distributions at $y = 950$ and $1,100$ were adopted as the angle dependence of the reflected light intensity for different Au film thickness, the maximum reflectivity change $(\Delta R/R)_{\max, \theta_2}$ was 0.656, and minimum reflectivity change $(\Delta R/R)_{\min, \theta_1}$ was -0.131 . The difference of the position showing $(\Delta R/R)_{\max, \theta_2}$ and $(\Delta R/R)_{\min, \theta_1}$ is 109 pixels (0.547°), so that FOM was $1.4^{\circ-1}$ for reflectivity change $\Delta R/R$, which is smaller than that ($2.7^{\circ-1}$) of the wedge-shaped Au thin film (I). The reason for the smaller FOM is that the minimum reflectivity is slightly larger at $y = 950$ of the wedge-shaped Au thin film (II) than that of (I). Further improvement requires the reduction of the minimum reflectivity by preparing a wedge-shaped Au thin film with a wider thickness range ($t_{\text{Au}} = 30\text{--}60$ nm), including the thickness showing the minimum reflectivity, than the wedge-shaped Au film (II).

DISCUSSION

It is important to reduce the minimum reflectivity by realizing the momentum matching condition by selecting the optimum thickness of the Au layer for the wavelength of the incident light in order to enhance the sharpness. It was found that thickness control of as small as 1 nm is necessary for satisfying

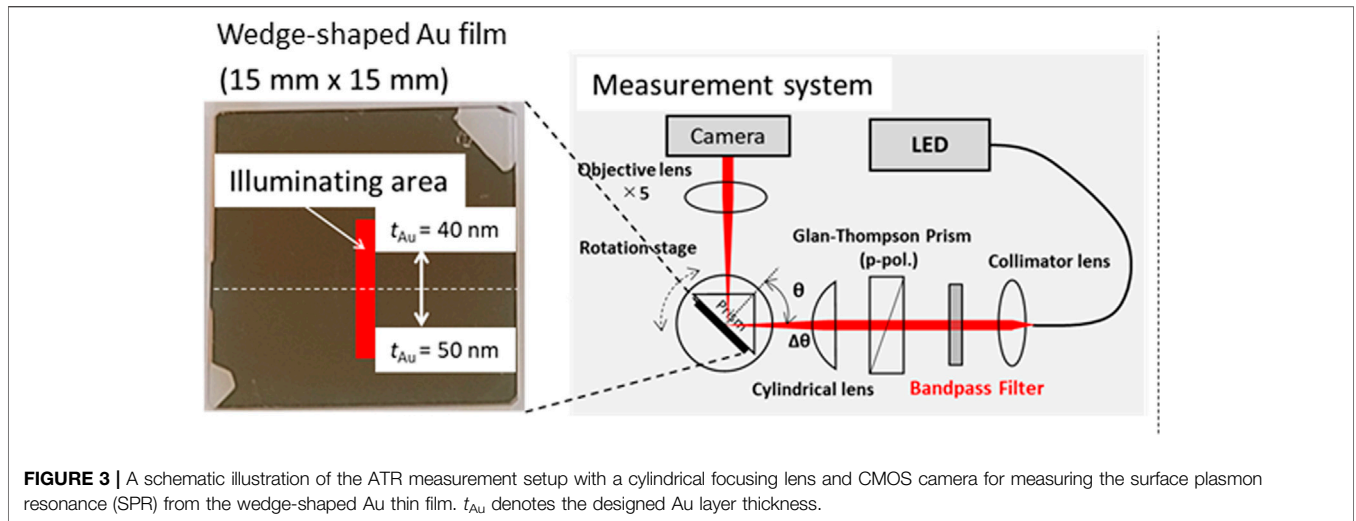


FIGURE 3 | A schematic illustration of the ATR measurement setup with a cylindrical focusing lens and CMOS camera for measuring the surface plasmon resonance (SPR) from the wedge-shaped Au thin film. t_{Au} denotes the designed Au layer thickness.

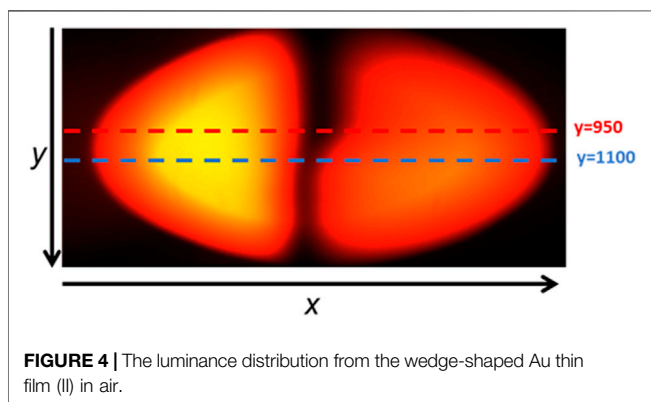


FIGURE 4 | The luminance distribution from the wedge-shaped Au thin film (II) in air.

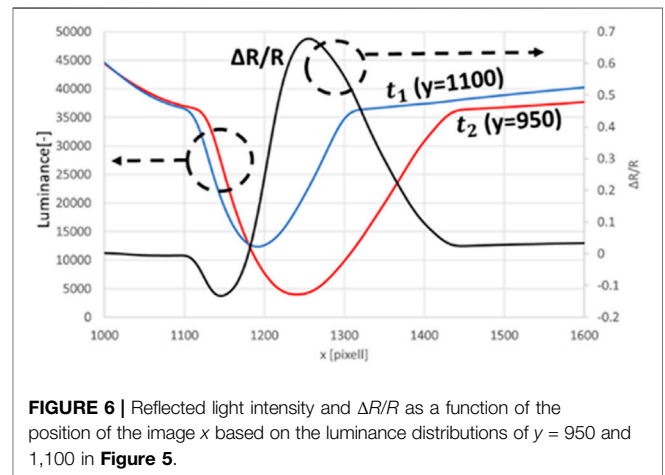


FIGURE 6 | Reflected light intensity and $\Delta R/R$ as a function of the position of the image x based on the luminance distributions of $y = 950$ and $1,100$ in **Figure 5**.

the condition. In the measurement setup in **Figure 3**, the minimum reflectivity was determined by the minimum luminance level (number of bits) and dark current of the CMOS camera, which are smaller than the minimum reflectivity observed in **Figure 4**. From the shift in position showing the minimum reflectivity along the y direction, the thickness resolution was determined by the nominal thickness

change (10 nm) divided by the difference in position (150 pixels), corresponding to 6.6×10^{-2} nm/pixel. It is possible to realize thickness control smaller than 0.1 nm without precise setting of the thickness during EB evaporation, which will contribute to the further enhancement of the FOM.

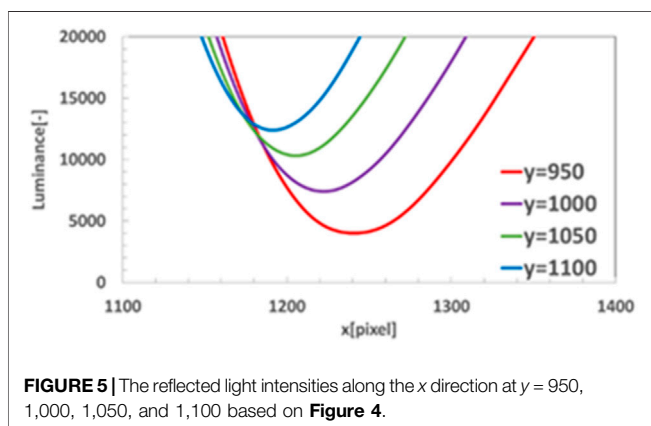
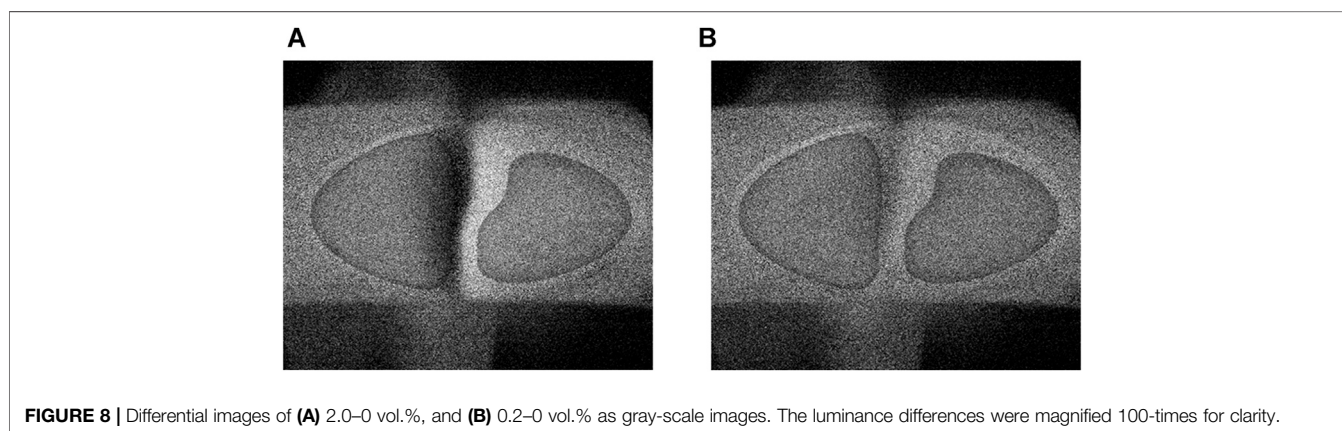
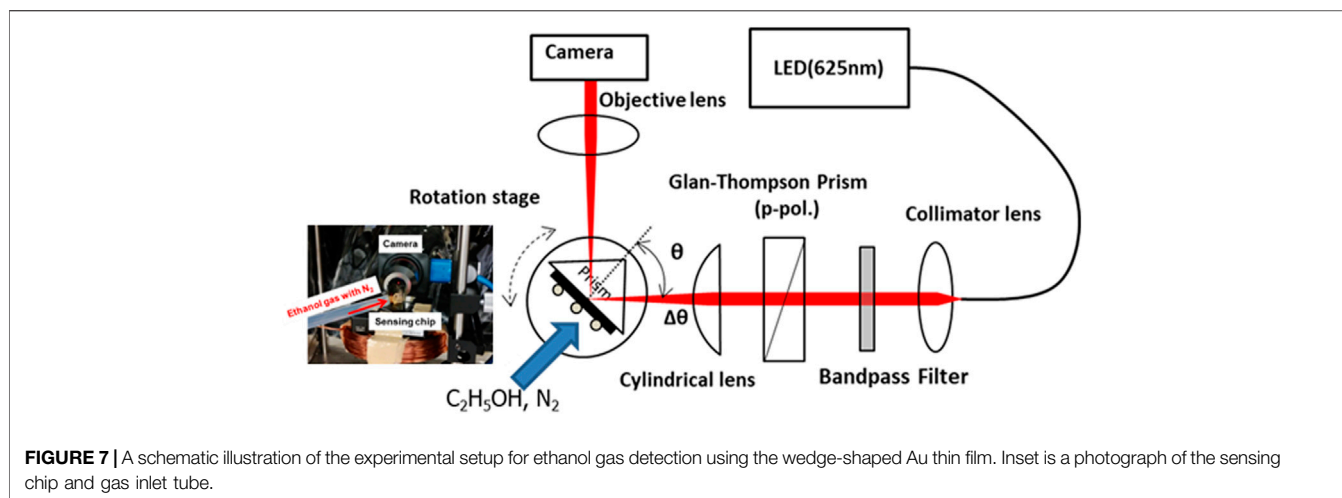


FIGURE 5 | The reflected light intensities along the x direction at $y = 950, 1,000, 1,050,$ and $1,100$ based on **Figure 4**.

SENSING CHARACTERISTICS OF TRANSDUCERS BASED ON A WEDGE-SHAPED AU THIN FILM

Measurement Setup and Difference in Images Upon Ethanol Gas Injection

We measured the ethanol gas sensing characteristics by using the wedge-shaped Au thin film (II) as a transducer without any surface functionalization. **Figure 7** shows a schematic diagram of the experimental setup for detecting the difference in the acquired images (distribution of the reflected light intensity) when ethanol gas was injected. We introduced diluted ethanol gas with a concentration of 0.2–2.0 vol.%, and observed the shift of the



SPR images. The ethanol gas was generated by a bubbler, which was composed by a flask filled with ethanol liquid and a gas inlet for N_2 gas injection. The generated ethanol gas was diluted by introducing another N_2 gas in order to control the concentration by changing the mixing ratio of the N_2 gas for generating ethanol gas and the N_2 gas for dilution. The diluted ethanol gas was introduced to the sample surface, while keeping the temperature of the ethanol liquid at 14°C , based on the saturation vapor concentration of 4 vol.% at 14°C . The total flow rate was kept constant at 2 L/min. Before changing the ethanol concentration, we introduced pure N_2 gas without ethanol for 1 min in order to desorb any ethanol molecules on the sample surface and purge the remaining ethanol gas inside the inlet tube. The concentration change of 0.2 vol.% corresponds to a refractive index change of 2×10^{-5} . We recorded an image under each ethanol gas concentration. **Figure 8** shows differential images of (A) 2.0–0 vol.%, and (B) 0.2–0 vol.% as grayscale images. The luminance differences were magnified 100-times to clarify them. White and black parts can be seen at the middle of the images corresponding to the reflectivity change owing to the surface plasmon resonance. The influences of the light intensity and mechanical drift were negligible in sensing these concentrations. The difference of the

images can be distinguished for the two concentrations. The results of quantitative evaluation will be given in the next sections.

Change in $\Delta R/R$ Upon Ethanol Gas Injection

We calculated the reflectivity changes $\Delta R/R$ when injecting ethanol gas and pure N_2 , based on the *Angular Dependence of Reflectivity in the Wedge-Shaped Au Thin Film in Attenuated Total Reflection Setup Based on Surface Plasmon Resonance Image* section, and investigated the influence of improved FOM for $\Delta R/R$ based on the wedge-shaped Au thin film (II). **Figure 9** shows $\Delta R/R$ for ethanol gas concentrations of 0–2.0 vol.%, as a function of the pixel position along the horizontal direction. **Figure 10** summarizes the change of $\Delta R/R$ [$\delta(\Delta R/R)$] as a function of the ethanol gas concentration. $\delta(\Delta R/R)$ monotonically increased with increasing concentration. The shift of the image Δx owing to the change of the angle showing minimum reflectivity by SPR is also plotted as a reference in **Figure 11**. The amount of shift Δx was averaged over five lines along the horizontal direction of the image and is thus not an integer, in order to read out the signal more precisely. $\delta(\Delta R/R)$ was distinguished for the concentrations of 0, 0.2, 0.6, 1.0, and 2.0 vol.%. The limit of detection was limited by the lowest concentration in the present ethanol gas generating

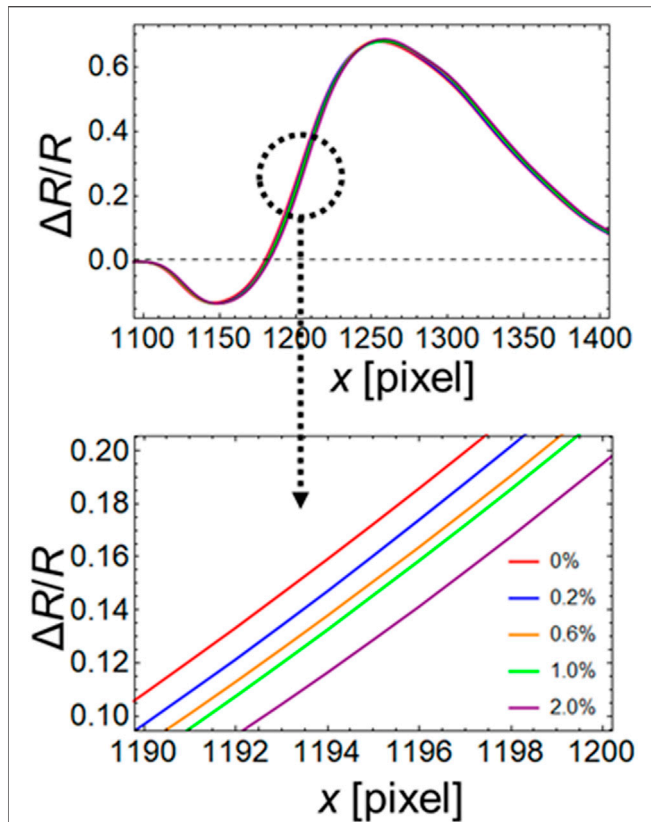


FIGURE 9 | $\Delta R/R$ for ethanol gas concentrations of 0–2.0 vol.% as a function of the pixel position along the horizontal direction.

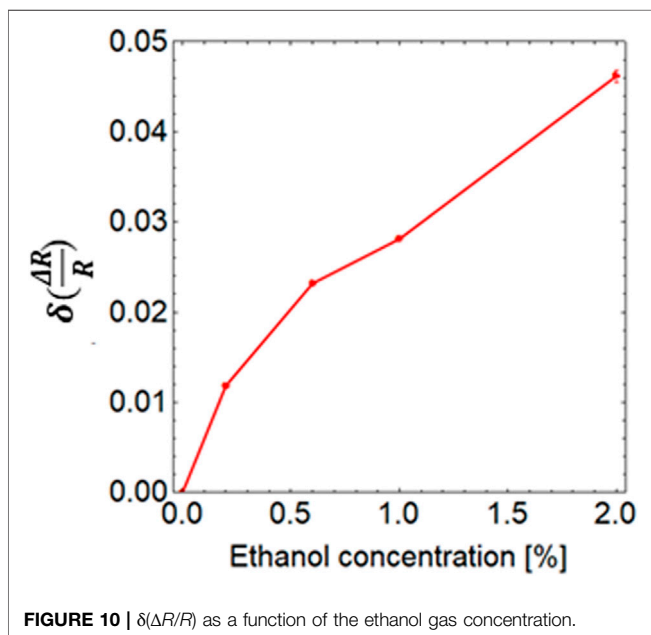


FIGURE 10 | $\delta(\Delta R/R)$ as a function of the ethanol gas concentration.

equipment, which was 0.2 vol.%. On the other hand, Δx was 1.4 pixels for 0.2 vol.%, which is close to an image shift of 1 pixel (a shift in incident angle of 0.005°). Therefore, $\Delta R/R$ gives a better

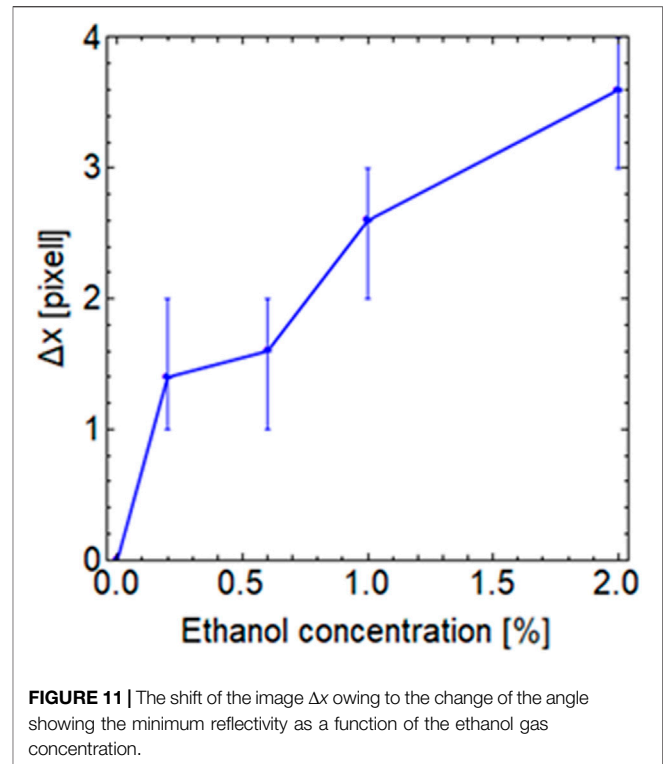


FIGURE 11 | The shift of the image Δx owing to the change of the angle showing the minimum reflectivity as a function of the ethanol gas concentration.

sensing magnitude with a wedge-shaped Au thin film than the angle showing the minimum reflectivity within the measurement setup.

CONCLUSION

We fabricated a wedge-shape Au thin film for modulating the wavenumber of surface plasmon polaritons by using the varying thickness of the Au in a single chip, in order to improve the thickness controllability for reducing the minimum reflectivity and to enhance the sharpness (FOM), defined as the normalized reflectivity change $\Delta R/R$ from the reflectivities at two positions on the Au thin film with two different thicknesses. With a combination of the wedge-shaped Au thin film, a focusing lens, and a CMOS camera, a thickness resolution as small as 6.6×10^{-2} nm/pixel was obtained, enabling improved thickness controllability. The maximum reflectivity change $\Delta R/R$ was 0.868, and the FOM was larger than that based on the reflectivity R , meaning that $\Delta R/R$ in the wedge-shaped Au thin film in this study results in a better sensing magnitude than R . Detection of ethanol gas at a minimum concentration of 0.2% (RI difference of 2×10^{-5}) was demonstrated without any functionalization. It is possible to improve $\Delta R/R$, the FOM, and RI sensitivity by preparing a wedge-shaped Au thin film with a wider thickness range. An SPR sensor based on a wedge-shaped Au thin film does not need external modulators or precise thickness control of the metal film and has a smaller footprint and higher sensitivity than conventional SPR sensors, and can therefore be applied to a wide range of sensing applications.

DATA AVAILABILITY STATEMENT

The original contributions presented in the study are included in the article, further inquiries can be directed to the corresponding author.

AUTHOR CONTRIBUTIONS

HS conceived and designed the project. TO, TM, and SS performed research concerning the optical simulations, preparations, and characterizations of wedge-shaped Au thin

films, and sensing characteristics. HS wrote the paper with input from all authors, and supervised the project.

FUNDING

This work was supported by the JSPS KAKENHI (Grant Numbers JP18K18851 and JP20K20996), the JST A-STEP (Grant Number JPMJTM20D1), the Murata Science Foundation, and the Casio Science Promotion Foundation, Japan.

REFERENCES

- David, S., Polonschii, C., Luculescu, C., Gheorghiu, M., Gáspár, S., and Gheorghiu, E. (2015). Magneto-plasmonic Biosensor with Enhanced Analytical Response and Stability. *Biosens. Bioelectron.* 63, 525–532. doi:10.1016/j.bios.2014.08.004
- Herreño-Fierro, C. A., Patiño, E. J., Armelles, G., and Cebollada, A. (2016). Surface Sensitivity of Optical and Magneto-Optical and Ellipsometric Properties in Magnetoplasmonic Nanodisks. *Appl. Phys. Lett.* 108, 021109. doi:10.1063/1.4939772
- Homola, J., Yee, S. S., and Gauglitz, G. (1999). Surface Plasmon Resonance Sensors: Review. *Sensors Actuators B: Chem.* 54, 3–15. doi:10.1016/s0925-4005(98)00321-9
- Kabashin, A. V., Patskovsky, S., and Grigorenko, A. N. (2009). Phase and Amplitude Sensitivities in Surface Plasmon Resonance Bio and Chemical Sensing. *Opt. Express* 17, 21191. doi:10.1364/oe.17.021191
- Kaiharu, T., Shimizu, H., Cebollada, A., and Armelles, G. (2016). Magnetic Field Control and Wavelength Tunability of SPP Excitations Using Al₂O₃/SiO₂/Fe Structures. *Appl. Phys. Lett.* 109, 111102. doi:10.1063/1.4962653
- Kaiharu, T., Shimodaira, T., Suzuki, S., Cebollada, A., Armelles, G., and Shimizu, H. (2019). Fe Thicknesses Dependence of Attenuated Total Reflection Response in Magnetoplasmonic Double Dielectric Structures: Angular versus Wavelength Interrogation. *Jpn. J. Appl. Phys.* 58, 122003. doi:10.7567/1347-4065/ab5205
- Liedberg, B., Nylander, C., and Lundström, I. (1995). Biosensing with Surface Plasmon Resonance - How it All Started. *Biosens. Bioelectron.* 10, i–ix. doi:10.1016/0956-5663(95)96965-2
- Liedberg, B., Nylander, C., and Lundström, I. (1983). Surface Plasmon Resonance for Gas Detection and Biosensing. *Sensors and Actuators* 4, 299–304. doi:10.1016/0250-6874(83)85036-7
- Maccaferri, N., E. Gregorczyk, K., de Oliveira, T. V. A. G., Kataja, M., van Dijken, S., Pirezadeh, Z., et al. (2015). Ultrasensitive and Label-free Molecular-Level Detection Enabled by Light Phase Control in Magnetoplasmonic Nanoantennas. *Nat. Commun.* 6, 6150. doi:10.1038/ncomms7150
- Manera, M. G., Ferreira-Vila, E., Garcia-Martin, J. M., Garcia-Martin, A., and Rella, R. (2014). Enhanced Antibody Recognition with a Magneto-Optic Surface Plasmon Resonance (MO-SPR) Sensor. *Biosens. Bioelectron.* 58, 114–120. doi:10.1016/j.bios.2014.02.003
- Markowicz, P. P., Law, W. C., Baev, A., Prasad, P. N., Patskovsky, S., and Kabashin, A. (2007). Phase-sensitive Time-Modulated Surface Plasmon Resonance Polarimetry for Wide Dynamic Range Biosensing. *Opt. Express* 15, 1745. doi:10.1364/oe.15.001745
- Patskovsky, S., Maisonneuve, M., Meunier, M., and Kabashin, A. V. (2008). Mechanical Modulation Method for Ultrasensitive Phase Measurements in Photonics Biosensing. *Opt. Express* 16, 21305. doi:10.1364/oe.16.021305
- Phillips, K. S. (2008). *Surface Plasmon Resonance-Based Sensors*. Berlin Heidelberg: Springer.
- Regatos, D., Fariña, D., Calle, A., Cebollada, A., Sepúlveda, B., Armelles, G., et al. (2010). Au/Fe/Au Multilayer Transducers for Magneto-Optic Surface Plasmon Resonance Sensing. *J. Appl. Phys.* 108, 054502. doi:10.1063/1.3475711
- Regatos, D., Sepúlveda, B., Fariña, D., Carrascosa, L. G., and Lechuga, L. M. (2011). Suitable Combination of noble/ferromagnetic Metal Multilayers for Enhanced Magneto-Plasmonic Biosensing. *Opt. Express* 19, 8336. doi:10.1364/oe.19.008336
- Sepúlveda, B., Calle, A., Lechuga, L. M., and Armelles, G. (2006). Highly Sensitive Detection of Biomolecules with the Magneto-Optic Surface-Plasmon-Resonance Sensor. *Opt. Lett.* 31, 1085. doi:10.1364/ol.31.001085
- Shimodaira, T., Suzuki, S., Aizawa, Y., Imura, Y., and Shimizu, H. (2019). “Surface Plasmon Resonance Transducers with Membrane Structure toward Gas-Sensing Applications,” in *Proc. SPIE 10926* (Bellingham, WA: Quantum Sensing and Nano Electronics and Photonics XVI), 1092628. doi:10.1117/12.2506852
- Shin, Y.-B., Kim, H. M., Jung, Y., and Chung, B. H. (2010). A New palm-sized Surface Plasmon Resonance (SPR) Biosensor Based on Modulation of a Light Source by a Rotating Mirror. *Sensors Actuators B: Chem.* 150, 1–6. doi:10.1016/j.snb.2010.08.006
- Suzuki, S., Maeda, T., Ogura, T., Suzuki, S., Kaiharu, T., and Shimizu, H. (2021). Modulation of Surface Plasmon Resonance by Magnetization Reversal in Au/Fe/Au Trilayer and Wedge Structure for Achieving Higher Refractive index Sensitivity. *Jpn. J. Appl. Phys.* 60, SB106. doi:10.35848/1347-4065/abea4b

Conflict of Interest: This study received funding from The Murata Science Foundation, and the Casio Science Promotion Foundation, Japan. The funders were not involved in the study design, collection, analysis, interpretation of data, the writing of this article or the decision to submit it for publication. All authors declare no other competing interests.

Publisher's Note: All claims expressed in this article are solely those of the authors and do not necessarily represent those of their affiliated organizations, or those of the publisher, the editors and the reviewers. Any product that may be evaluated in this article, or claim that may be made by its manufacturer, is not guaranteed or endorsed by the publisher.

Copyright © 2021 Shimizu, Ogura, Maeda and Suzuki. This is an open-access article distributed under the terms of the Creative Commons Attribution License (CC BY). The use, distribution or reproduction in other forums is permitted, provided the original author(s) and the copyright owner(s) are credited and that the original publication in this journal is cited, in accordance with accepted academic practice. No use, distribution or reproduction is permitted which does not comply with these terms.